Theses of Doctoral (PhD) Dissertation

STUDYING BIOAVAILABILITY OF RED AND GREY NANO-SELENIUM IN ANIMAL MODELS

Aya Ferroudj
Ph.D. candidate

Supervisor:
Dr. József Prokisch PhD
professor

UNIVERSITY OF DEBRECEN

Doctoral School of Animal Science

Debrecen, 2026

1. BACKGROUND, JUSTIFICATION AND AIM OF THE STUDY

Nanotechnology offers innovative approaches to improve animal production by enhancing growth performance, feed efficiency, health status, and product quality. In poultry nutrition, nanoparticles improve nutrient bioavailability and enable controlled release, while also providing antimicrobial effects that may reduce reliance on antibiotics. Nano-minerals such as selenium, silver, copper, and iron have demonstrated potential to enhance antioxidant defense, immune function, growth, and reproductive performance. Selenium plays a vital role in antioxidant protection, thyroid hormone metabolism, and reproduction through its incorporation into selenoproteins, including glutathione peroxidases and thioredoxin reductases. However, conventional inorganic selenium sources suffer from limited bioavailability and narrow safety margins. Selenium nanoparticles (SeNPs) have therefore emerged as promising alternatives, offering improved bioavailability, reduced toxicity, and enhanced biological efficacy. At the nanoscale, selenium's surface reactivity and particle characteristics strongly influence absorption, tissue distribution, and metabolism. Elemental selenium exists primarily in two allotropes: amorphous red and crystalline grey forms, which differ in structural stability and reactivity. While grey selenium is often considered biologically inert based on bulk selenium studies, this assumption may not apply at the nanoscale, where particle size and crystallinity can preserve biological activity. Comparative data on red and grey SeNPs, particularly regarding bioavailability, antioxidant function, and tissue targeting, remain limited. The Japanese quail (Coturnix japonica) is a suitable avian model for nutritional studies due to its rapid growth, efficient feed conversion, and sensitivity to oxidative stress. Therefore, this study aimed to evaluate the bioavailability and biological activity of red amorphous and grey crystalline selenium nanoparticles in vivo and to determine whether structural transformation from red to grey SeNPs alters selenium metabolism, antioxidant defense, and organ-specific deposition in poultry.

- Synthesize red (amorphous) and grey (crystalline) selenium nanoparticles and confirm their structural distinction at the nanoscale, using complementary physicochemical techniques (SEM–EDS, XRD, Raman spectroscopy, and fluorescence analysis), to verify that the materials differ in allotropy while retaining identical elemental composition.
- Investigate the influence of selenium nanoparticle allotropy on in vivo selenium metabolism, by comparing red and grey selenium nanoparticles with respect to bioavailability, tissue distribution, antioxidant activity, and post-withdrawal kinetics in adult male Japanese quails.

- Examine dose-dependent selenium retention and depletion after dietary withdrawal, in order to determine how selenium nanoparticle allotropy and the transformation of red selenium into the more stable grey form influence selenium bioavailability, biological efficacy, and the practical stability (shelf life) of nano-selenium.

2. MATERIALS AND METHODS

2.1. Production and Characterization of Selenium nanoparticles

Red amorphous selenium nanoparticles (SeNPs) were synthesized by chemical reduction of sodium selenite using ascorbic acid in aqueous solution under continuous stirring at room temperature. The formation of red SeNPs was confirmed by the characteristic red coloration of the suspension. After centrifugation and washing, the nanoparticles were freeze-dried. Grey crystalline SeNPs were obtained by thermal transformation of red SeNPs at 85 °C for 10 min. Nanoparticle morphology and elemental composition were examined using scanning electron microscopy coupled with energy-dispersive X-ray spectroscopy (SEM–EDS). Structural differences between red and grey SeNPs were confirmed by X-ray diffraction (XRD) and Raman spectroscopy. Fluorescence spectroscopy was applied to assess excitation-dependent emission behavior, while selenium concentrations were determined by atomic fluorescence spectrometry (AFS) following acid digestion.

2.3. Animal experiments

2.3.1. General Husbandry and Dietary Management

All animal experiments were conducted at the University of Debrecen, Hungary, and approved by the institutional Ethics Committee (permission No. 4/2021/DEMÁB). Adult male Japanese quails (Coturnix japonica) were housed individually under controlled environmental conditions (25 ± 2 °C; 16 h light/8 h dark) with ad libitum access to drinking water. Birds received a basal diet formulated according to NRC (1994) recommendations, containing a background selenium level of 0.21 mg/kg. Selenium nanoparticles were homogeneously incorporated into the diets to achieve the required supplementation levels.

2.3.2. First Animal Experiment: Growth Performance and Tissue Selenium Distribution

The first experiment was a 28-day feeding trial conducted on 20 adult male Japanese quails (11 weeks of age). Birds were randomly allocated into five dietary groups (n = 4): control (no SeNPs), red SeNPs at 0.26 or 0.71 mg/kg, and grey SeNPs at 0.26 or 0.71 mg/kg. Body weight and feed intake were recorded daily. At the end of the experiment, birds were euthanized and samples of liver, spleen, kidney, testis, breast muscle, eyes, and blood were collected. Organs were weighed to calculate organ indices. All samples were washed with phosphate-buffered saline and stored at −80 °C until selenium analysis by atomic fluorescence spectrometry.

2.3.3. Second Animal Experiment: Antioxidant Status and Selenium Retention/Depletion

The second experiment involved 60 adult male Japanese quails (12 weeks of age) assigned to five dietary treatments (n = 12): control (no SeNPs), red SeNPs at 0.71 or 5.21 mg/kg, and grey SeNPs at 0.71 or 5.21 mg/kg. Birds were fed the experimental diets for 28 days. Thereafter, half of the birds from each group were sampled, while the remaining birds underwent a 7-day selenium-free withdrawal period before final sampling. Tissue samples (liver, kidney, spleen, testis, breast muscle, eyes, and blood) were collected at days 28 and 35. Blood samples were centrifuged to obtain serum and red blood cell fractions. Selenium retention and depletion were calculated by comparing tissue selenium concentrations before and after the withdrawal period.

2.3.3.1. Antioxidant Biomarker Analysis

Antioxidant status was evaluated by measuring glutathione peroxidase (GSH-Px), superoxide dismutase (SOD), and total antioxidant capacity (T-AOC) in liver homogenates and serum samples. Commercial colorimetric assay kits were used according to the manufacturers' protocols, and absorbance was measured using a microplate reader.

2.3.3.2. Statistical analysis

Data are presented as mean ± SEM. Results from the first experiment were analyzed using one-way ANOVA, while data from the second experiment were evaluated using one- or two-way ANOVA, depending on the experimental design. Differences among means were assessed using Fisher's or Tukey's post hoc tests. Statistical significance was accepted at $p < 0.05$.

3. RESULTS

3.1. Selenium nanoparticles production

The chemical reduction of sodium selenite with ascorbic acid resulted in the successful formation of selenium nanoparticles, as evidenced by the development of a distinct reddish colouration in the reaction mixtures. The appearance of this colour indicated the formation of colloidal red selenium nanoparticles and was observed consistently for all prepared concentrations. The red SeNPs suspensions remained visually stable during the reaction period, with no apparent precipitation at low concentrations of 0.05, 0.5, and 5 mg/L. Upon thermal treatment of the red SeNPs suspensions at 85 °C for 10 min, a clear colour change from red to grey was observed, confirming the transformation of amorphous red selenium into the grey selenium allotrope. This visual transition was reproducible across all batches, indicating effective allotrope conversion under the applied conditions. After purification and freeze-drying, the red SeNPs were obtained as reddish solid powders, whereas the grey SeNPs formed dark grey to black powders, demonstrating that the characteristic colour differences were preserved in the solid state. Representative images showing the visual appearance of selenium nanoparticles in suspension and after freeze-drying are presented. The marked differences between the red and grey forms provide qualitative confirmation of successful synthesis and thermal transformation prior to further physicochemical characterization.

3.2. Characterization of Selenium nanoparticles allotropes

The physicochemical and optical properties of red and grey selenium nanoparticles (SeNPs) were systematically investigated using a combination of scanning electron microscopy (SEM), particle size analysis, energy-dispersive X-ray spectroscopy (EDS), X-ray diffraction (XRD), Raman spectroscopy, and fluorescence spectroscopy. This multi-technique approach was employed to elucidate allotrope-dependent differences in morphology, structure, elemental composition, and optical behaviour.

3.2.1. SEM-EDS analysis

To examine allotrope-dependent differences in morphology and particle dimensions, scanning electron microscopy (SEM) was employed to characterize the surface structure and size distribution of red and grey selenium nanoparticles **Figures 1-2.**

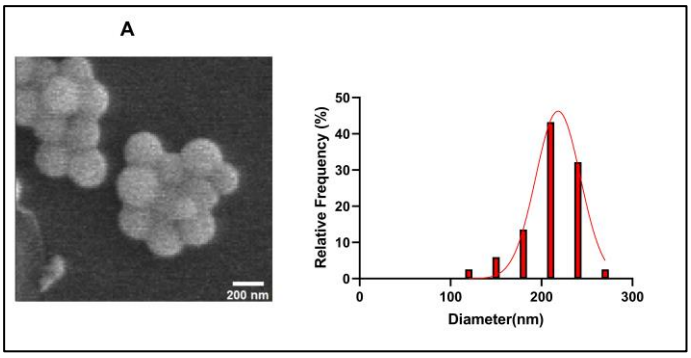

Figure 1: SEM Images of: (A) red SeNPs and diameter distribution histogram

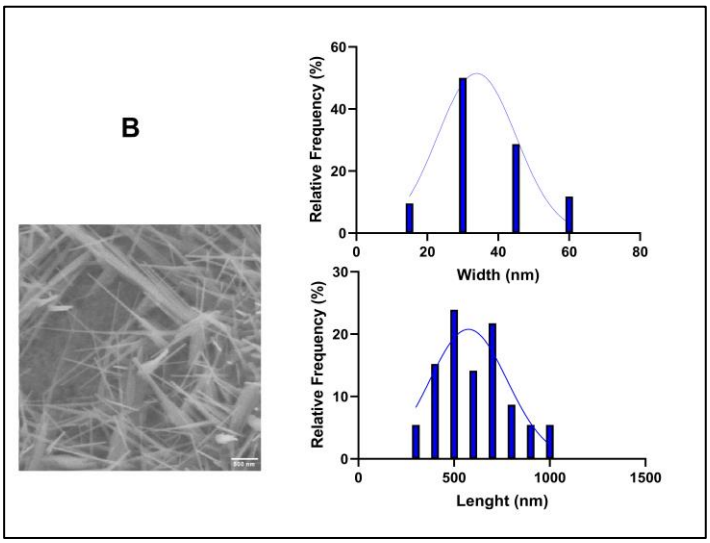

Figure 2: SEM Images of: (B) grey SeNPs and length and width distribution histograms

SEM analysis revealed clear morphological distinctions between the two selenium nanoparticle allotropes. Red SeNPs showed a quasi-spherical to spherical morphology, forming compact aggregates of smooth, non-faceted primary particles with a narrow size distribution (mean diameter 218 ± 24 nm), characteristic of amorphous systems produced under kinetically controlled reduction where isotropic nucleation dominates due to the absence of long-range atomic order (Khandsuren & Prokisch, 2021a, 2021b; Li, Zhu, et al., 2024; Tendenedzai et al., 2022)SEM analysis revealed clear morphological distinctions between the two selenium nanoparticle allotropes. Red SeNPs showed a quasi-spherical to spherical morphology, forming compact aggregates of smooth, non-faceted primary particles with a narrow size distribution (mean diameter 218 ± 24 nm), characteristic of amorphous systems produced under kinetically controlled reduction where isotropic nucleation dominates due to the absence of long-range atomic order (Khandsuren & Prokisch, 2021a, 2021b; Li et al., 2024; Tendenedzai et al., 2022). In contrast, grey SeNPs exhibited a highly anisotropic, needle-like structure, forming interconnected networks of elongated nanocrystals with mean lengths of 575 ± 202 nm and

widths averaging 33.9 ± 11 nm. This pronounced aspect ratio reflects directional crystal growth along the helical Se–Se chains typical of the trigonal crystalline lattice, confirming the successful thermal transformation of amorphous red SeNPs into crystalline grey SeNPs (Chellapa et al., 2020; Khandsuren & Prokisch, 2021a; L. Ren et al., 2004), Following morphological characterization, energy-dispersive X-ray spectroscopy (EDS) was used to verify the elemental composition and assess the purity of both red and grey selenium nanoparticles **Figure 3.**

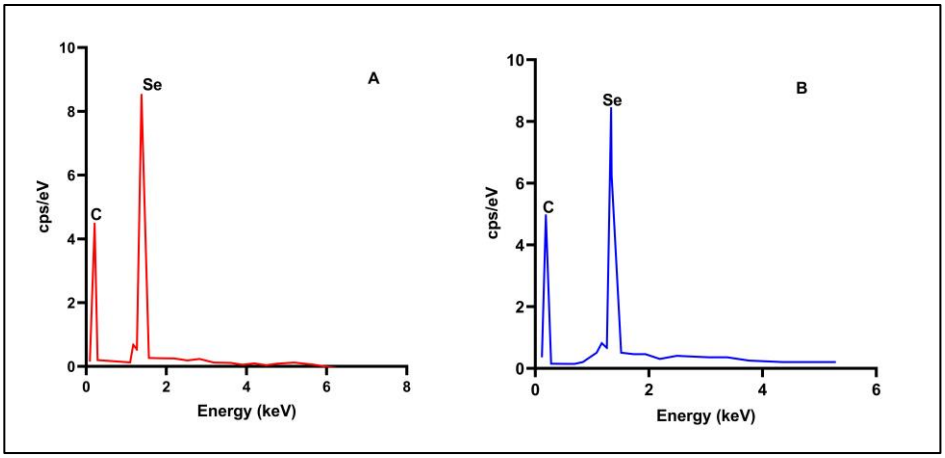

Figure 3: EDS spectra of (A) red SeNPs and (B) grey SeNPs

EDS analysis confirmed selenium as the dominant elemental constituent in both red and grey SeNPs, with a characteristic Se Lα peak at ~1.37 keV observed in all spectra. A carbon signal was also detected, which can be attributed to the carbon substrate used during SEM–EDS analysis. No additional elemental impurities were detected within the sensitivity limits of the technique, indicating comparable elemental purity for both allotropes. Importantly, EDS confirmed that the observed differences between red and grey SeNPs arise from structural and morphological variations rather than elemental composition.

3.2.2. XRD analysis

To determine the structural nature and crystallinity of the synthesized selenium nanoparticles, X-ray diffraction (XRD) analysis was performed on both allotropes **Figure 4.**

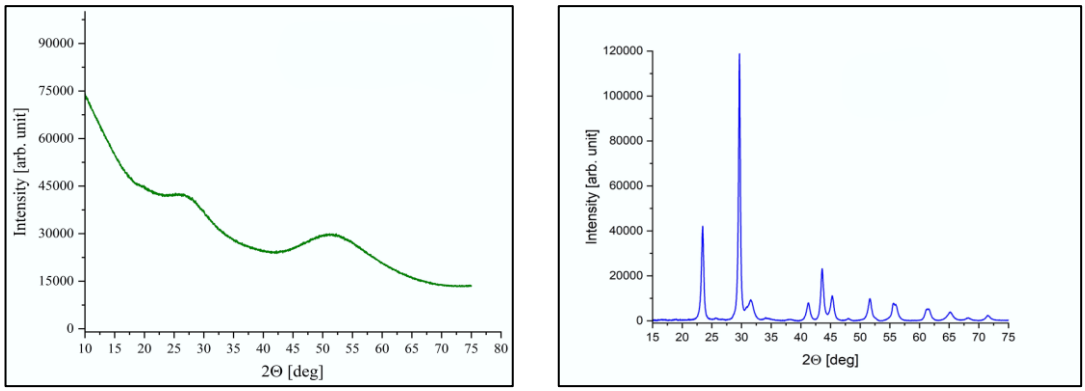

Figure 4: XRD patterns of (A) red SeNPs and (B) grey SeNPs

XRD analysis revealed a fundamental structural distinction between the two selenium allotropes. The diffraction pattern of red SeNPs was characterized by broad, diffuse scattering features and the absence of sharp Bragg reflections, indicating an amorphous structure with no long-range atomic order. A weak hump in the 20–30° 2θ range was attributed to short-range atomic correlations typical of amorphous selenium. In contrast, grey SeNPs exhibited multiple sharp and intense diffraction peaks across the scanned 2θ range, corresponding to crystalline trigonal selenium (t-Se). The narrow peak widths and high intensities confirmed a high degree of crystallinity and long-range periodicity. No amorphous halos or secondary phases were observed, indicating a complete transformation to the crystalline grey allotrope. These findings are in excellent agreement with previous reports describing amorphous red selenium and crystalline trigonal grey selenium nanostructures(Alex et al., 2024; Fardsadegh et al., 2019; Y. Wang et al., 2012; Xi et al., 2006; Xiong et al., 2006). Together with SEM results, the XRD patterns demonstrate that the two SeNPs systems differ fundamentally in atomic ordering, which underlies their distinct morphologies.

3.2.3. Raman spectroscopy

Raman spectra of selenium are presented in the **Figure 5,** confirming structural differences between red and grey SeNPs. The red SeNPs exhibited characteristic and weak peaks in the range of 250–255 cm^{-1}, which are typically associated with the amorphous state of selenium, where structural disorder leads to peak broadening and poorly resolved vibrational modes. In contrast, the grey SeNPs showed distinct peaks between 230–235 cm^{-1}, corresponding to the A_1 vibrational mode of trigonal selenium associated with Se–Se stretching along helical chains. The narrow linewidth and high intensity of this peak indicate well-ordered atomic arrangements, in excellent agreement with the crystalline structure identified by XRD.

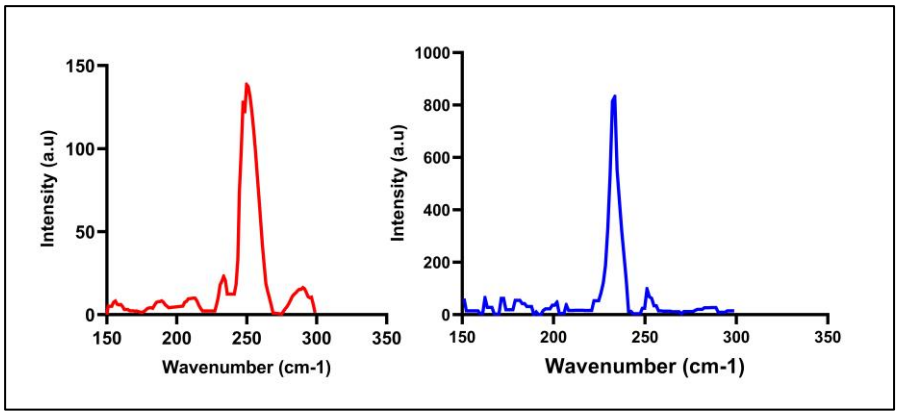

Figure 5: Raman spectra of Selenium (redline) Red Se. (blueline) Grey Se

Similar Raman features for amorphous and crystalline selenium have been reported previously (Anupama et al., 2021; Baganich et al., 1991; Goldan et al., 2016; Kizovský et al., 2021; Tugarova et al., 2018); the amorphous phase typically shows Raman bands around 250 cm^{-1}, while crystalline selenium occurs in two polymorphic forms: pure trigonal structure, characterized by the ~233-237 cm^{-1} band observed in this study, and the monoclinic crystals, which appear near 251 cm^{-1}. Raman spectroscopy, therefore, provides strong complementary evidence for the allotrope-dependent structural states of the synthesized SeNPs. The sensitivity of selenium Raman bands to environmental and oxidative conditions further reflects the redox-active nature of selenium (Lopez et al., 1981), emphasizing the usefulness of Raman spectroscopy in distinguishing selenium phases at the nanoscale.

3.2.4. Fluorescence analysis

The optical properties of the amorphous red selenium nanoparticles and crystalline grey selenium nanoparticles were further investigated using excitation–emission fluorescence spectroscopy to evaluate their electronic and surface-related states **Figure 6-7.**

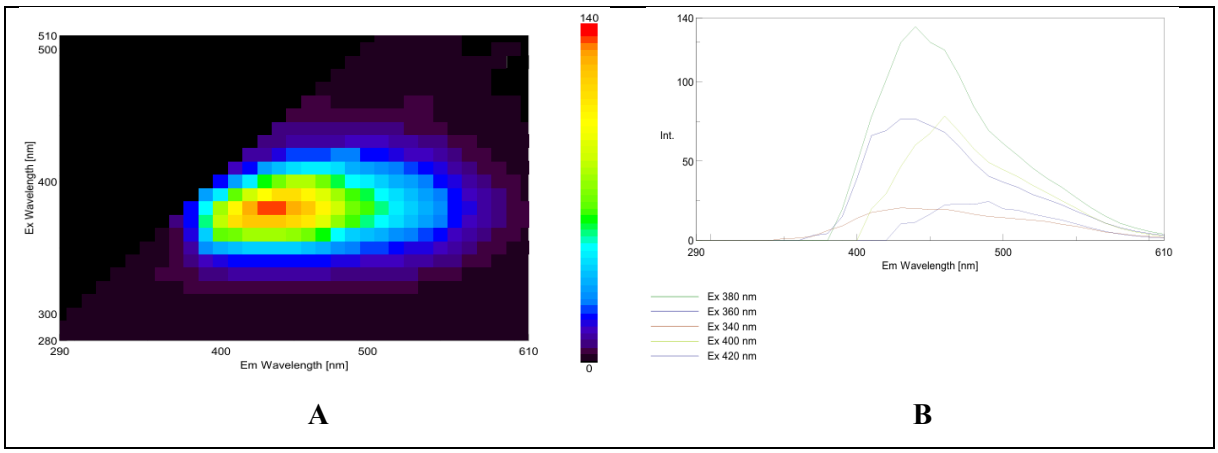

Figure 6: Fluorescence characteristics of red SeNPs at 1000 mg/L: (A) 3D excitation–emission fluorescence spectrum of red SeNPs, and (B) 2D emission spectra recorded at different excitation wavelengths

The fluorescence characteristics of red SeNPs at 1000 mg/L were evaluated using full scan fluorescence analysis **Fig. 6-A**. A weak fluorescence region was observed with the maximum emission around 430–450 nm when excited at ~380 nm. The emission spectra recorded at selected excitation wavelengths **Fig. 6-B** confirmed this behaviour, with the highest fluorescence intensity obtained at 380 nm excitation, followed by moderate signals at 360 nm and 400 nm, while 340 nm and 420 nm resulted in comparatively weaker emissions. The overall low intensity highlights the limited optical response of red SeNPs, distinguishing them from grey SeNPs, which displayed stronger fluorescence under similar conditions.

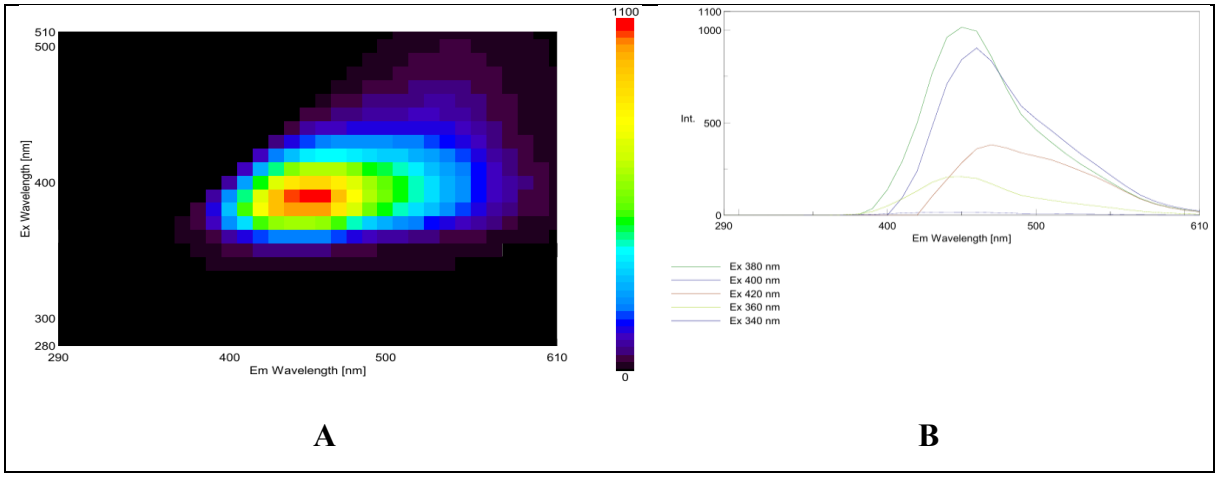

Figure 7: Fluorescence characteristics of grey SeNPs at 1000 mg/L: (a) 3D excitation–emission fluorescence spectrum of grey SeNPs, and (b) 2D emission spectra recorded at different excitation wavelengths

The fluorescence characteristics of grey SeNPs at 1000 mg/L were evaluated using full scan fluorescence analysis **Fig. 7-A**. A well-defined fluorescence region was observed with the maximum emission centred around 430–450 nm when excited at ~380–400 nm, indicating strong optical activity in the blue region. The emission spectra recorded at selected excitation wavelengths **Fig. 7-B** confirmed this behaviour, with the highest fluorescence intensity obtained at 380 nm excitation, followed closely by 400 nm, while 420 nm, 360 nm, and 340 nm resulted in comparatively weaker emissions. The variation in intensity across excitation wavelengths highlights the excitation-dependent optical response of grey SeNPs. This behaviour is consistent with the strong optical activity of grey SeNPs, distinguishing them from red SeNPs, which exhibit lower fluorescence intensity under similar conditions. The optical properties of the SeNPs further support their nanoscale character. Biosynthesized SeNPs showed strong fluorescence activity in the 398–420 nm range, with excitation at 398 nm and emission intensities exceeding 800 a.u. (Tripathi et al., 2020). Red SeNPs additionally exhibited an absorption band in the UV–Vis spectrum at ~260–270 nm, confirming their distinct optical activity (Shahzamani et al., 2022). Such photoluminescence behaviour is strongly size- and

surface-dependent, and selenium species are known to emit across the visible to near-infrared range (J. Wang et al., 2023). Notably, red SeNPs have been reported to fluoresce near the NIR region, making them suitable for biomedical applications such as imaging, diagnostics, and intracellular tracking (Khalid et al., 2016). For comparison, selenite itself typically emits at ~475 nm (Song et al., 2013), highlighting the altered optical behaviour of nano selenium. However, the literatures indicate that crystalline selenium nanostructures can indeed display significant fluorescence. For example,(Gates et al., 2002) observed optical activity in trigonal selenium nanowires, and a more recent work demonstrated that selenium quantum dots with a trigonal structure exhibit strong solid-state fluorescence, with emission peaks varying between 418–449 nm depending on excitation wavelength (Anupama et al., 2021).

3.2.5. Concentration-Dependent Fluorescence Response

Fluorescence measurements were performed on red and grey selenium nanoparticles (SeNPs). Fluorescence intensity was measured across a concentration range of Se (0–1000 mg/L) in the sample solution **Figure 8**.

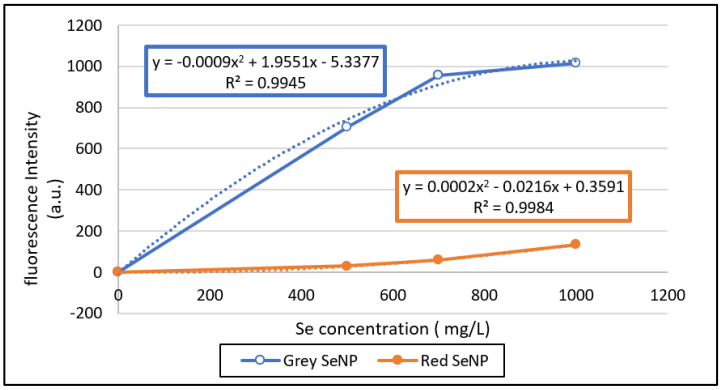

Figure 8: Fluorescence Intensity of Grey and Red Selenium Nanoparticles at Different Concentrations (mg/L)

Grey SeNPs exhibited a concentration-dependent increase in fluorescence intensity, reaching a maximum near 1000 mg/kg, with the relationship well described by a quadratic fit ($R^2 = 0.9945$). In contrast, red SeNPs showed only a marginal increase in fluorescence intensity across the tested concentrations, with considerably lower emission compared to grey SeNPs ($R^2 = 0.9984$). These findings highlight the stronger optical activity and concentration sensitivity of grey SeNPs relative to red SeNPs, suggesting distinct structural or surface-state contributions to their fluorescence behaviour (Anupama et al., 2021; Gates et al., 2002).

3.3. First Animal Experiment: Growth Performance and Tissue Selenium Distribution

3.3.1. Growth performance

Figure 9 exhibits the final live body weight of Japanese quails fed diets supplemented with varying amounts of dietary nano-Se. The body weight was significantly affected by the nanoparticle treatments, as indicated by the statistical differences between groups; the group with treatment 2 (0.5 red nano-Se) achieved the highest BW average The control group (C0) showed an intermediate value and did not differ significantly from T2 or T4 as indicated by the statistical overlapping. The T1 and T3 groups (0.05 mg/kg red and grey SeNPs) exhibited lowest body weights. These results indicate that selenium nanoparticle supplementation influenced body weight in a dose- and form-dependent manner rather than consistently improving growth performance across all treatments..

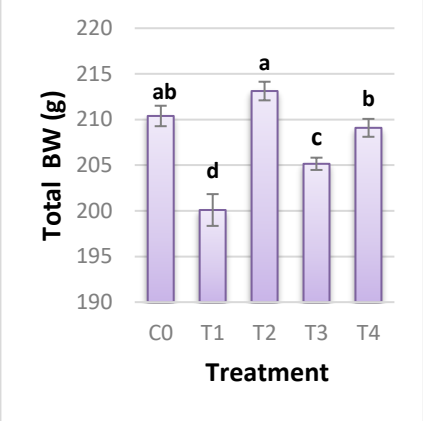

Figure 9: Influence of Different Levels of Selenium Nanoparticles (SeNPs) Dietary Supplementation on the live body weight (g) ± SEM of Adult Japanese Quails. Means with the differing letters are Significantly Different ($p < 0.05$). C0: control; T1: 0.05 mg/kg Red SeNP; T2: 0.5 mg/kg Red SeNP; T3: 0.05 mg/kg Grey SeNP; T4: 0.5 mg/kg Grey SeNP

The feed intake was measured daily during the 28-day trial for the five groups treated with SeNPs supplements. **Figure 10** of total feed intake showed that the feed intake is not significantly affected by the various selenium doses and forms. All groups consumed comparable amounts of food; that indicates that Se did not influence the birds' appetite and feed consumption patterns. However, in the present study, although feed intake remained unchanged among treatments, moderate selenium nanoparticle supplementation did not produce a consistent improvement in body weight compared with the control group.

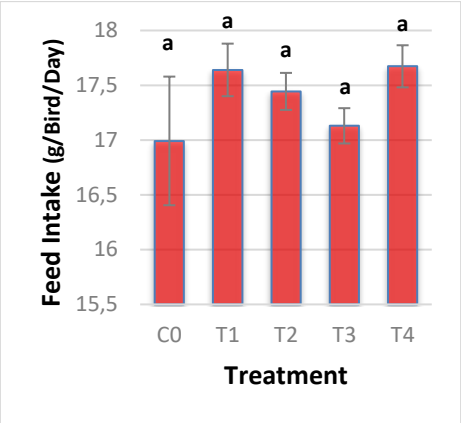

Figure 10: Impact of Different Doses of Selenium Nanoparticles (SeNPs) Dietary Supplementation on the Average feed intake (g) ± SEM of Adult Japanese Quails. Means with the Same letter Are Not Significantly Different ($p > 0.05$). C0: control; T1: 0.05 mg/kg Red SeNP; T2: 0.5 mg/kg Red SeNP; T3: 0.05 mg/kg Grey SeNP; T4: 0.5 mg/kg Grey SeNP.

Nano selenium supplementation of Japanese quails (Coturnix japonica) with 0.5 mg/kg in red and grey forms and with 0.05 mg/kg Grey Se produced treatment-dependent differences in body weight; however, these differences did not consistently result in higher body weight compared with the control group. This agrees with the research results of (Elkhateeb et al., 2024; Kaewsatuan et al., 2024; Marković et al., 2018; Reda et al., 2024; Tsekhmistrenko et al., 2020), which reveal better growth rates in avian species: quails, chickens and broiler treated with nanoparticles of Se between the ranges of 0.2, 0.3, 0.4 and 0.6 mg/kg. Meanwhile, the recommended level of Se is 0.15 mg/kg in poultry feeding (National Research Council, 1994). However, the 0.05 mg/kg of selenium group showed signs of Se deficiency, such as reduced body weight boost, Selenite and nano-amorphous selenium may utilize the same transporters or absorption pathways (Sindireva et al., 2023). This overlap could lead to competition at the cellular or intestinal level, potentially resulting in a physiological response similar to selenium deficiency, even under supplementation (Bakke et al., 2010; Schiavon & Pilon-Smits, 2017). It was found that nanoelement Se has an identical effect in layer chicks where the growth performance was impaired at a level of 0.3 mg/kg (Mohapatra et al., 2014). The body weight alterations were most observed due to improved nutrient utilization rather than feed consumption. Comparable trend has been reported by Biswas et al. (2006) and Kaewsatuan et al. (2024) where selenium treatment enhanced feed efficiency while not affecting total feed intake across all treatments.

3.3.2. Organ Indices

The liver index presented in **Fig. 11-A** had a notable variation among the groups treated with SeNPs ($p < 0.05$). The highest values were recorded in treatment 1 (0.05 Red nano-Se), followed by the lowest values in Treatment 2 (0.5 Red nano-Se), T3 (0.05 Grey nano-Se) and T4 (0.5 Grey nano-Se), while The control group (C0) showed an intermediate value and did not differ significantly from any of the treatments. **Fig. 11-B** showed the spleen relative weights, where there are no significant differences across all treatments ($p > 0.05$).

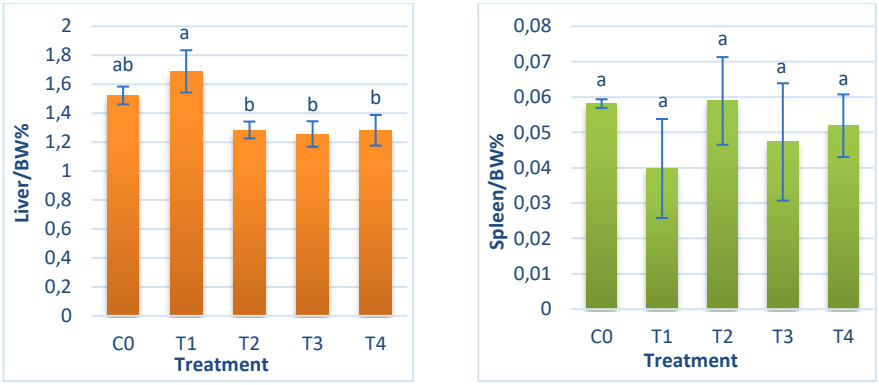

A B

Figure 11: Effects of Dietary Selenium Nanoparticle Supplementation on Liver (A) and Spleen (B) weights (Relative to Body Weight) in Adult Japanese Quails ± SEM. Means with the Same superscript are Not Significantly Different ($p > 0.05$) while means with different letters are Significantly Different ($p < 0.05$). C0: control; T1: 0.05 mg/kg Red SeNP; T2: 0.5 mg/kg Red SeNP; T3:0.05 mg/kg Grey SeNP; T4: 0.5 mg/kg Grey SeNP

The liver and spleen indices, representing organ weight relative to body weight, serve as indicators of organ function and potential toxicity (Long et al., 2021; Z. Ren et al., 2022). Studies have shown that glycine nano-selenium caused no significant changes in these indices, confirming its non-toxic nature (Z. Ren et al., 2022). Similarly, nano- and inorganic selenium had no adverse effects on heart, liver, or digestive organs in broiler quails, though young quails in the fattening phase showed a slight liver index increase with nano-selenium supplementation (Khazraei et al., 2022; Alagawany et al., 2021). The spleen index remained within the normal range (0.04–0.06%), indicating no immune or tissue damage (Abdel-Moneim et al., 2020; Biswas et al., 2006). However, chick quails exhibited a moderate rise in lymphoid organ weights (1.8–3%), likely due to enhanced selenium absorption and targeted immune tissue delivery (Khazraei et al., 2022).

3.3.3. Organ-Specific Selenium Uptake

Selenium (Se) distribution varied across tissues depending on the treatment group and tissue type (**Fig.12 A–F**).

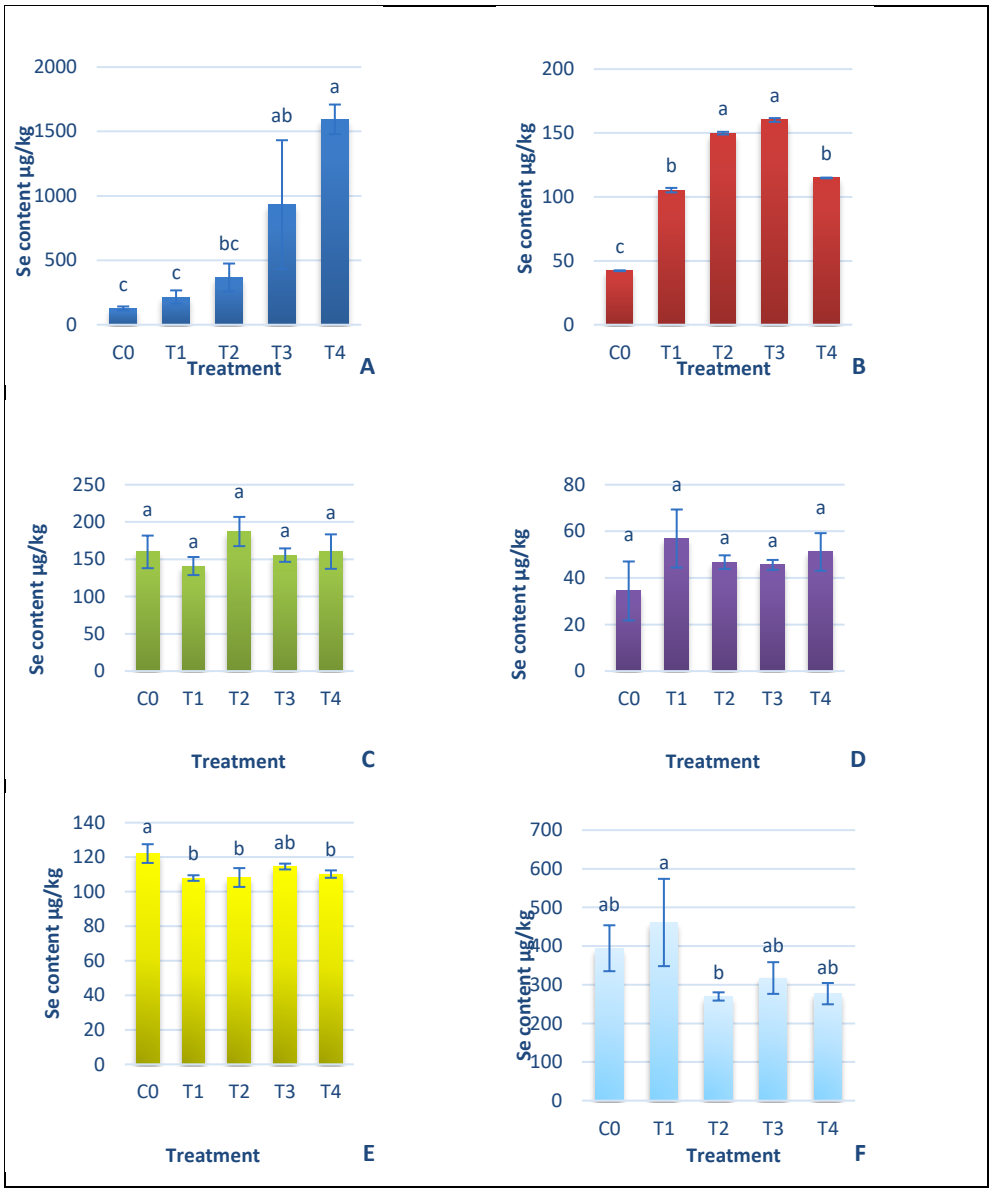

Figure 12: Nanoparticle of Selenium distribution on Liver (A), red Blood cellular fraction (B), Kidneys (C), Testis (D) and Eyes (E), and Breast (F). Means ± SEM with the Same Superscript Are Not Significantly Different ($p > 0.05$), while means with different letters are Significantly Different ($p < 0.05$). C0: control; T1: 0.05 mg/kg Red SeNP; T2: 0.5 mg/kg Red SeNP; T3: 0.05 mg/kg Grey SeNP; T4: 0.5 mg/kg Grey SeNP

Selenium deposition in quail tissues revealed dose- and form-dependent patterns with values well below established toxicity thresholds (0.15–0.50 mg/kg) for poultry (Commission Implementing Regulation (EU), 2022; National Research Council, 1994). Liver selenium increased significantly with supplementation, reaching the highest levels in grey SeNPs (0.5 mg/kg), confirming the liver's role in selenium metabolism and storage (Marković et al., 2018; Reda et al., 2024). The greater retention in grey SeNP-treated groups suggests higher bioavailability and particle stability (Filipović et al., 2021). Red blood cell Se also rose notably in both red and grey SeNP groups, supporting selenium's role in oxidative stress regulation and

erythropoiesis via glutathione peroxidase (GPx) activity (Dehkordi et al., 2017; Sadeghian et al., 2012). Conversely, kidney and testis Se levels remained stable, indicating effective homeostatic control that prevents toxic buildup (Hadrup & Ravn-Haren, 2023). although other studies suggest nano-selenium can enhance reproductive Se content in mammals and birds (Abdelnour et al., 2021; Kazaz et al., 2020). Ocular selenium showed little variation, consistent with findings in avian and human studies showing tightly regulated Se levels to avoid excess accumulation (Christen et al., 2015; McFarland et al., 1970). In breast muscle, Se deposition was modest and variable, with low-dose red SeNPs showing the highest incorporation, possibly reflecting saturation mechanisms limiting further uptake (Gawor et al., 2020; Zhou & Wang, 2011). Overall, both selenium nanoparticle forms enhanced Se bioavailability without toxicity, indicating efficient absorption, regulated distribution, and tissue-specific selenium homeostasis, consistent with prior reports of nano-selenium's superior biological efficiency (Kralik et al., 2012; Mahmoud et al., 2024; Zoidis et al., 2014).

3.4. Second Animal Experiment

3.4.1. Growth Performance

Dietary supplementation with red or grey SeNPs did not significantly affect feed intake and body weight progress throughout the 28-day feeding period ($p > 0.05$) **(Fig.13-14)**. The mean FI presented in **Figure 13** remained comparable between the control and all supplemented groups, including the high-dose treatments (5 mg/kg), indicating normal feeding behaviour and the absence of overt selenium-induced anorexia.

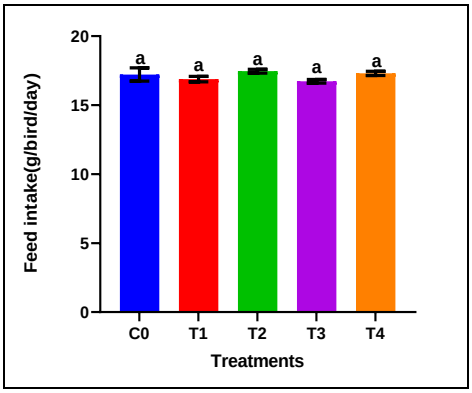

Figure 13: Feed intake of adult male Japanese quails during 28 days of dietary supplementation with selenium nanoparticles (n=6). Values are presented as mean ± SEM. No significant differences were observed among treatments ($p > 0.05$)

The body weight of Japanese quails at Week 1 and Week 4 in the second animal experiment is presented in **Fig.14.** At the beginning of the supplementation period (Week 1), no significant

differences in body weight were observed among the experimental groups, indicating a homogeneous initial distribution of birds. After four weeks of feeding with diets supplemented with red or grey selenium nanoparticles at 0.5 and 5 mg/kg, body weight had no statistically significant differences been detected between the control and any of the SeNPs-treated groups ($p > 0.05$).

These results demonstrate that dietary supplementation with selenium nanoparticles, irrespective of allotrope form or dose, did not significantly influence body weight during the experimental period. This suggests that the applied SeNPs levels were physiologically safe and did not exert growth-promoting or growth-depressing effects under the present conditions. Similar observations have been reported in previous studies, where selenium supplementation primarily affected antioxidant status and selenium deposition in tissues rather than overall growth performance when basal diets already met selenium requirements(Mahmoud et al., 2024; Mohapatra et al., 2014).

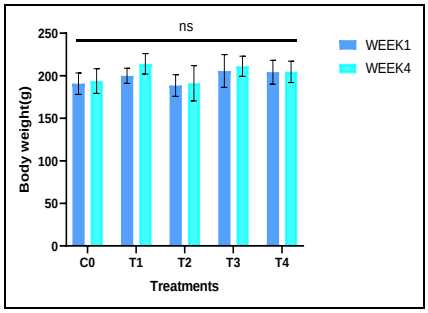

Figure 14: Body weight of Japanese quails in the second animal experiment at Week 1 and Week 4 under different dietary selenium nanoparticle treatments. C0: control diet without SeNPs; T1: 0.5 mg/kg red SeNPs; T2: 5 mg/kg red SeNPs; T3: 0.5 mg/kg grey SeNPs; T4: 5 mg/kg grey SeNPs. Bars represent mean ± SEM. No significant differences among treatments were detected (ns, $p > 0.05$)

3.4.2. Selenium distribution among Tissues

Table 1 shows the selenium distribution in organs of Japanese quails and total selenium content after 28 days for both allotropes of SeNPs supplementation. Selenium concentrations varied significantly among treatments and organs ($p < 0.0001$). The red SeNPs treatments (T1 and T2) resulted in higher selenium concentrations in several metabolically active tissues, with the highest values observed in the T2 group. In this group, selenium levels reached 263.18 µg/kg ± 26 in red blood fractions, 128.86 µg/kg ± 1.6 in the liver, and 196.93 µg/kg ± 6.2 in breast muscle, indicating a dose-dependent increase for red SeNPs. The lower red SeNPs dose (T1) also increased selenium concentrations in the spleen, RBFs and breast compared with the control. Grey SeNPs supplementation showed a distinct accumulation pattern. The low dose

(T3) resulted in lower selenium concentrations in the spleen and testis while maintaining comparable breast muscle selenium levels to the red SeNPs groups. At the higher dose (T4), grey SeNPs produced marked increases specifically in the spleen and testis, whereas liver selenium levels were comparable to those observed in T2. Kidney selenium concentrations varied moderately among treatments, with a significant elevation only observed in the T2 group relative to the control. Selenium concentrations in the eyes remained relatively stable across all treatments. Moreover, the high-dose groups T2 and T4 showed higher total Se levels compared with the control. Overall, the groups supplemented with nanoparticles of selenium produced the highest selenium accumulation and distribution in different organs; grey SeNPs demonstrated a strong dose dependence, with substantial increases observed only at higher concentrations in the spleen and testis.

Table 1: Selenium distribution in organs of Japanese quails and average selenium content after 28 days of control and SeNPs supplementation (n=6)

Se Content ($\mu g.kg^{-1}$)	C	T1	T2	T3	T4	*p* Value
Spleen	49.3±1.6 ^{c}	76.3±6.6 ^{b}	67.7±4.6 ^{b}	39.1±1.02^{d}	135.2±3.8 ^{a}	<0.0001
Kidney	101.3±3.7 ^{b}	91.2±4.4 ^{b}	114.8±1.5 ^{a}	93.4±2.8 ^{b}	89.6±4.4 ^{b}	<0.0001
Testis	119±5.3 ^{b}	112.4±2.5 ^{b}	124.2±3.1 ^{b}	93.5±4.3 ^{c}	151±7.2 ^{a}	<0.0001
Eyes	220.4±7.1 ^{a}	214.7±6.9 ^{a}	240.8±7.7 ^{a}	213.4±6.9 ^{a}	222.1±4.5 ^{a}	<0.0001
RBF (red blood fraction)	166.5± 4.9^{c}	195.9±6.7 ^{b}	263.2±27 ^{a}	160.8± 4 ^{c}	162.4±3.8 ^{c}	<0.0001
Breast muscle	178.8±1.5 ^{b}	186.6±1.6 ^{ab}	196.9±6.2 ^{a}	183.2±2.3 ^{ab}	192.1±9.7 ^{ab}	<0.0001
Liver	96.4±2.3 ^{b}	93.1±1.9 ^{b}	128.9±1.6 ^{a}	92.6±7 ^{b}	110.7±7.5 ^{ab}	<0.0001
Average Se content	133.1± 3.8^{b}	138.6±4.3 ^{b}	162.3±6.9 ^{a}	125.1±3.9 ^{b}	151.9±5.7 ^{a}	0.0007

Data are presented as mean ± SEM. Different superscript letters within each row indicate statistically significant differences among dietary treatments ($p < 0.05$). Total selenium content was analyzed separately; asterisks indicate significant differences compared with the control (*** $p < 0.001$), while ns denotes non-significant differences.

Selenium distribution varied markedly between red and grey SeNPs (0.5 mg/kg) **Fig. 15**. In the red SeNP group (T1), selenium was highest in the eyes, followed by the red blood fraction (RBF) and breast muscle, with lower but uniform levels in the liver, kidney, spleen, and testis, indicating balanced systemic deposition. Conversely, in the grey SeNP group (T3), selenium followed the order eyes > breast muscle = RBF > liver = kidney = testis > spleen, with the lowest levels in the spleen, suggesting reduced selenium accumulation in immune and circulating tissues. Overall, red SeNPs promoted broader selenium distribution, while grey SeNPs showed more selective, organ-dependent deposition, consistent with differences in bioavailability and tissue affinity.

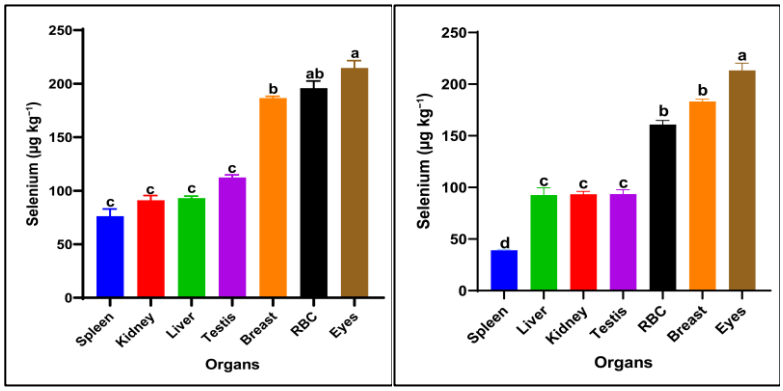

(a) **(b)**

Figure 15: Selenium distribution in spleen, kidney, liver, testis, breast muscle, red blood cells (RBCs), and eyes of Japanese quails supplemented with red SeNPs ((**a**): T1, 0.5 mg/kg) and grey SeNPs ((**b**): T3, 0.5 mg/kg). Bars represent mean ± SEM. Different superscript letters within each treatment indicate significant differences in selenium concentration among organs ($p < 0.05$)

3.4.3. Antioxidant Biomarkers

After 28 days of supplementation, selenium nanoparticles (SeNPs) markedly influenced antioxidant enzyme activity in quails **Fig. 16**. Hepatic glutathione peroxidase (GPx) activity increased significantly in all high-dose groups, with the highest values in T2 (red SeNPs, 5 ppm) and T4 (grey SeNPs, 5 ppm), confirming a dose-dependent enhancement of GPx-mediated antioxidant defense. Liver superoxide dismutase (SOD) remained stable across treatments, while serum SOD decreased significantly in all SeNP-treated birds compared to controls, suggesting reduced oxidative stress and lower systemic demand for SOD activity. Liver total antioxidant capacity (TAC) was unchanged, but serum TAC varied significantly, peaking in T2 (red SeNPs, 5 ppm) and T3 (grey SeNPs, 0.5 ppm). Overall, red SeNPs at 5 ppm produced the strongest improvement in antioxidant status, enhancing both hepatic GPx activity

and serum TAC, while grey SeNPs showed slightly lower bioefficacy at high doses, indicating form- and dose-dependent antioxidant effects consistent with selenium bioavailability trends.

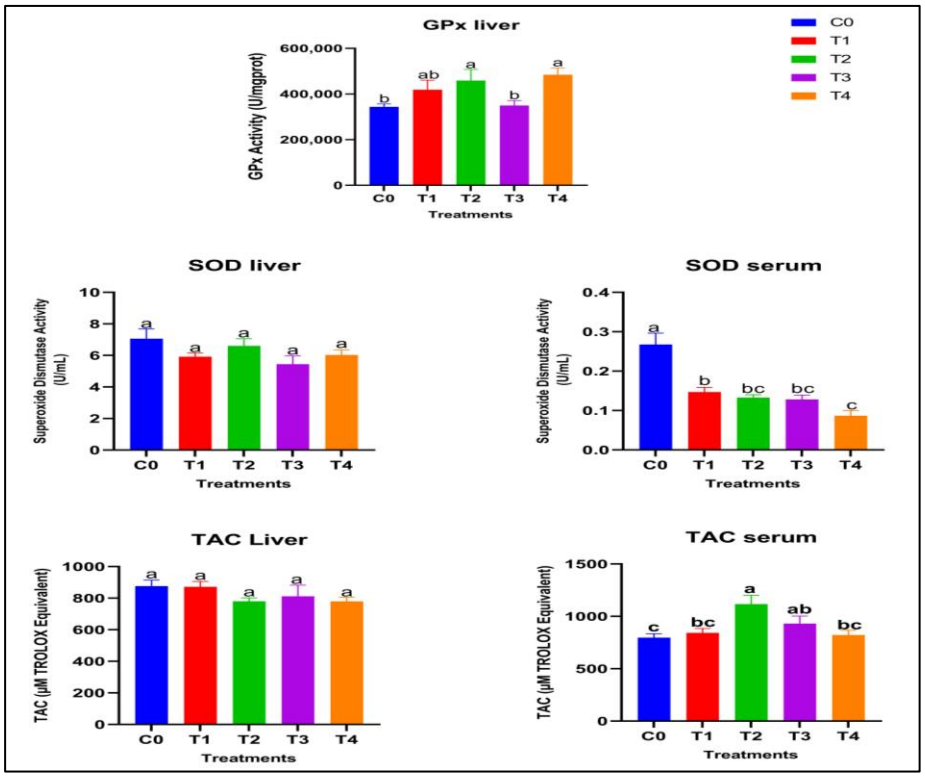

Figure 16: Antioxidant biomarkers in liver and serum of Japanese quails fed diets supplemented with selenium nanoparticles (SeNPs). Data are presented as mean ± SEM. Different superscript letters indicate statistically significant differences among dietary treatments ($p < 0.05$)

3.4.4. Selenium Retention after Withdrawal & Selenium Depletion Patterns

Table 2 shows the total retention and depletion rate (in liver, kidney, spleen and red blood fraction RBF). The total selenium retention and depletion percentages revealed clear treatment-dependent patterns. Control birds exhibited the most stable selenium balance (96% retention, 3.9% depletion), reflecting normal homeostatic regulation. Among the supplemented groups, the low-dose treatments (T1 and T3) achieved the highest overall retention (91% and 88%, respectively), indicating efficient incorporation and stable maintenance of selenium during the withdrawal period. In contrast, higher doses (T2 and T4) showed markedly lower retention (78% and 57%). This drop is a direct consequence of the body reaching tissue saturation, which subsequently triggers enhanced excretion and biological regulatory mechanisms to rapidly clear the excess selenium once supplementation is withdrawn. Red SeNPs displayed higher initial bioavailability and retention overall (T1 was 91%), while grey SeNPs followed closely in

second place, confirming that both nanoparticle forms lead to efficient selenium incorporation, but the clearance rate was primarily governed by the dose.

Table 3: Total selenium retention and depletion rates in Japanese quails following SeNPs supplementation and a 7-day withdrawal period

	C	T1	T2	T3	T4
TOTAL Se RETENTION %	96%	91%	78%	88%	57%
TOTAL Se DEPLETION %	4%	9%	22%	12%	43%

This study confirmed that selenium nanoparticles (SeNPs) exerted form- and dose-dependent effects on selenium metabolism, antioxidant activity, and retention in adult male Japanese quails(Ferroudj et al., 2025; Malik et al., 2025; Urbankova et al., 2021). Red SeNPs, particularly at 5 mg/kg (T2), produced the highest selenium deposition in metabolic and circulating compartments (liver, RBF, muscle), reflecting their greater solubility and bioavailability (Ashraf. S.S., 2021; Filipović et al., 2021). This was accompanied by enhanced hepatic GPx activity and serum TAC, demonstrating rapid selenium utilization for antioxidant enzyme synthesis (Guleria et al., 2020). Despite supranutritional dosing, no toxicity symptoms were observed, consistent with selenium's safe range for poultry (Burk & Hill, 2015). Conversely, grey SeNPs showed slower, more selective accumulation, with low-dose treatment (T3) achieving sustained retention and high-dose (T4) leading to saturation and post-withdrawal depletion, indicating homeostatic regulation of excess selenium (Ye et al., 2022). Low-dose red SeNPs (T1) achieved the highest retention (91%), suggesting superior long-term stability (Loeschner et al., 2014). Selenium distribution was tissue-specific: the eyes consistently held the highest Se levels, supporting their antioxidant demands (Christen et al., 2015), while the spleen and testis accumulated more selenium in grey SeNP groups, consistent with targeted immune and reproductive functions (Amini & Mahabadi, 2018). Overall, red SeNPs were more effective for rapid antioxidant enhancement and systemic distribution, whereas grey SeNPs provided controlled, prolonged release and organ-specific deposition, emphasizing that moderate dosing optimizes bioavailability and safety (Selmani et al., 2024; Tışlı et al., 2024).

4. CONCLUSIONS, RECOMMENDATIONS

This study explored how the allotropy of selenium nanoparticles (SeNPs) "specifically red (amorphous) and grey (crystalline) forms" affects their physicochemical characteristics and biological performance in adult male Japanese quails. By integrating material characterization and controlled feeding experiments, the research established clear structure–function relationships linking nanoparticle form to selenium bioavailability, tissue distribution, antioxidant response, and post-withdrawal kinetics. Physicochemical analyses confirmed successful synthesis of two distinct allotropes. Red SeNPs were quasi-spherical and amorphous, averaging 218 ± 24 nm in diameter, while grey SeNPs exhibited anisotropic, needle-like crystalline morphology (575 ± 202 nm length, 33.9 ± 11 nm width). X-ray diffraction and Raman spectroscopy verified the amorphous and trigonal crystal structures, respectively, while fluorescence analysis showed enhanced excitation-dependent emission for grey SeNPs, reflecting their ordered atomic structure. These findings demonstrated that selenium's nanoscale architecture—not composition alone—governs its physical and optical behaviour. Biologically, both SeNP forms were metabolically active and safe for poultry use but displayed distinct dynamics. Red SeNPs acted as a rapidly bioavailable selenium source, promoting higher selenium deposition in the liver, blood, and muscle and enhancing hepatic glutathione peroxidase and total antioxidant capacity. Grey SeNPs showed slower and selective accumulation, particularly in spleen and testis, suggesting a distinct physiological behaviour rather than biological inactivity. Selenium retention was dose dependent: moderate levels (0.5 mg/kg) achieved optimal retention (≈91% red, 88% grey), while supranutritional levels reduced retention due to homeostatic clearance. Tissue-specific regulation was evident—selenium preferentially accumulated in liver, muscle, and ocular tissues but remained tightly controlled in kidney and reproductive organs. Growth performance and feed intake were not adversely affected by selenium nanoparticle supplementation in either experiment, even at the highest dietary levels applied. The results confirm that nanostructure controls selenium metabolism, influencing absorption rate, tissue targeting, and antioxidant utilization. Red amorphous SeNPs provide faster systemic availability and stronger antioxidant support, while grey crystalline SeNPs function as slower and selective selenium reservoirs. Overall, this work demonstrates that selenium nanoparticle allotropy is a key determinant of bio functionality in poultry. By revealing how structural differences translate into metabolic and physiological outcomes, it offers a mechanistic foundation for precision nano-selenium supplementation aimed at improving poultry health, product quality, and nutritional biofortification potential.

5. NEW SCIENTIFIC RESULTS

2. In adult male Japanese quails, supplementation with amorphous red and crystalline grey selenium nanoparticles resulted in markedly different biological responses, including selenium bioavailability red SeNPs increased mean of tissue selenium to 162.3 µg/kg, whereas grey SeNPs reached 151.9 µg/kg, tissue distribution, antioxidant activity, and post-withdrawal kinetics, demonstrating that selenium nanoparticle allotropy governs in vivo selenium metabolism.
2. Grey crystalline selenium nanoparticles accumulated in specific organs at 5 mg/kg, particularly the spleen increased from 49.3 to 135.2 µg/kg and testis selenium from 119.0 to 151.0 µg/kg, and affect hepatic glutathione peroxidase activity depending on dosage, indicating biological activity rather than inertness.
3. Red amorphous SeNPs produced the highest selenium concentrations in metabolically active tissues. At 5 mg/kg, selenium increased to 263.2 µg/kg in the red blood fraction, 128.9 µg/kg in the liver, and 196.9 µg/kg in breast muscle and enhance antioxidant capacity suggesting their effectiveness as a selenium source.
4. After dietary withdrawal, moderate red and grey selenium nanoparticle supplementation (0.5 mg/kg) resulted in the highest selenium retention approximately 91% and 88% of selenium, respectively, whereas supranutritional doses led to accelerated selenium depletion to 22% and 43% respectively, demonstrating a clear dose-dependent regulation of selenium homeostasis and showing that higher intake does not ensure sustained selenium status.
5. Selenium deposition followed organ-specific and form-dependent patterns, with preferential accumulation of red selenium nanoparticles in metabolically active tissues (+34% in liver, +58% in blood, and +10% in muscles) and targeted deposition of grey selenium nanoparticles in spleen (+174%) and testis (+27%), revealing regulated, allotrope-dependent selenium targeting in Japanese quails.

6. PRACTICAL RESULTS

1) Red amorphous selenium nanoparticles showed high bioavailability and strong antioxidant efficacy; therefore, they can be applied as an efficient selenium source to rapidly improve selenium status and antioxidant defence in poultry, particularly under intensive production or oxidative stress conditions.
2) The demonstration that grey crystalline selenium nanoparticles are bioactive rather than inert indicates that they may serve as stable, sustained-release selenium sources. The red-to-grey transformation does not eliminate biological activity, supporting the practical feasibility and shelf stability of nano-selenium supplements.
3) The dose-dependent retention and clearance patterns indicate that moderate supplementation levels ensure the most efficient selenium utilization, whereas excessive doses lead to increased clearance and reduced long-term efficiency. This provides a practical basis for optimizing dietary selenium inclusion.
4) The organ-specific selenium targeting suggests that nanoparticle form can be selected according to physiological needs, with red SeNPs favouring systemic tissues and grey SeNPs supporting immune- and reproduction-related organs.
5) The absence of adverse effects on growth performance and feed intake confirms that selenium nanoparticles can be safely incorporated into poultry diets under controlled conditions, supporting their potential use in commercial feed formulations.
6) Finally, this study provides a scientific basis for further research on nano-selenium, including investigations of gene expression and molecular mechanisms, particularly selenoprotein- and antioxidant-related pathways, to clarify how nanoparticle allotropy regulates selenium metabolism. The results also support extending this approach to other poultry species and livestock. Moreover, exploring combined supplementation strategies, such as selenium nanoparticles with vitamin E or other bioactive compounds at varying doses, may reveal synergistic effects and improve nutritional efficiency.

7. REFERENCES

1) Abdel-Moneim, A.-M. E., Sabic, E. M., Abu-Taleb, A. M., & Ibrahim, N. S. (2020). Growth performance, hemato-biochemical indices, thyroid activity, antioxidant status, and immune response of growing Japanese quail fed diet with full-fat canola seeds. *Tropical Animal Health and Production*, *52*(4), 1853–1862. https://doi.org/10.1007/s11250-020-02200-1
2) Abdelnour, S. A., Alagawany, M., Hashem, N. M., Farag, M. R., Alghamdi, E. S., Hassan, F. U., Bilal, R. M., Elnesr, S. S., Dawood, M. A. O., Nagadi, S. A., Elwan, H. A. M., ALmasoudi, A. G., & Attia, Y. A. (2021). Nanominerals: Fabrication Methods, Benefits and Hazards, and Their Applications in Ruminants with Special Reference to Selenium and Zinc Nanoparticles. *Animals*, *11*(7), Article 7. https://doi.org/10.3390/ani11071916
3) Alagawany, M., Qattan, S. Y. A., Attia, Y. A., El-Saadony, M. T., Elnesr, S. S., Mahmoud, M. A., Madkour, M., Abd El-Hack, M. E., & Reda, F. M. (2021). Use of Chemical Nano-Selenium as an Antibacterial and Antifungal Agent in Quail Diets and Its Effect on Growth, Carcasses, Antioxidant, Immunity and Caecal Microbes. *Animals*, *11*(11), Article 11. https://doi.org/10.3390/ani11113027
4) Alex, A., Biju, T. S., Francis, A. P., Veeraraghavan, V. P., Gayathri, R., & Sankaran, K. (2024). Quercetin-coated biogenic selenium nanoparticles: Synthesis, characterization, and in-vitro antioxidant study. *Advances in Natural Sciences: Nanoscience and Nanotechnology*, *15*(1), 015012. https://doi.org/10.1088/2043-6262/ad2c7a
5) Amini, S. M., & Mahabadi, P. (2018). Selenium nanoparticles role in organ systems functionality and disorder. *Nanomedicine Research Journal*, *3(3)*, 117–124. https://doi.org/10.22034/nmrj.2018.03.001
6) Anupama, K., Paul, T., & Ann Mary, K. A. (2021). Solid-State Fluorescent Selenium Quantum Dots by a Solvothermal-Assisted Sol–Gel Route for Curcumin Sensing. *ACS Omega*, *6*(33), 21525–21533. https://doi.org/10.1021/acsomega.1c02441
7) Ashraf. S.S. (2021). Selenium-based amorphous semiconductors and their application in biomedicine. In *Electronic Devices, Circuits, and Systems for Biomedical Applications* (pp. 25–46). Academic Press. https://doi.org/10.1016/B978-0-323-85172-5.00017-4
8) Baganich, A. A., Mikla, V. I., Semak, D. G., Sokolov, A. P., & Shebanin, A. P. (1991). Raman Scattering in Amorphous Selenium Molecular Structure and Photoinduced Crystallization. *Physica Status Solidi (b)*, *166*(1), 297–302. https://doi.org/10.1002/pssb.2221660133
9) Bakke, A. M., Tashjian, D. H., Wang, C. F., Lee, S. H., Bai, S. C., & Hung, S. S. O. (2010). Competition between selenomethionine and methionine absorption in the intestinal tract of green sturgeon (*Acipenser medirostris*). *Aquatic Toxicology*, *96*(1), 62–69. https://doi.org/10.1016/j.aquatox.2009.09.014

10) Biswas, A., Mohan, J., & Sastry, K. V. H. (2006). Effect of higher levels of dietary selenium on production performance and immune responses in growing Japanese quail. *British Poultry Science*, *47*(4), 511–515. https://doi.org/10.1080/00071660600830629

11) Burk, R. F., & Hill, K. E. (2015). Regulation of Selenium Metabolism and Transport. *Annual Review of Nutrition*, *35*(1), 109–134. https://doi.org/10.1146/annurev-nutr-071714-034250

12) Chellapa, L. R., Shanmugam, R., Indiran, M. A., & Samuel, S. R. (2020). Biogenic nanoselenium synthesis, its antimicrobial, antioxidant activity and toxicity. *Bioinspired, Biomimetic and Nanobiomaterials*, *9*(3), 184–189. https://doi.org/10.1680/jbibn.19.00054

13) Christen, W. G., Glynn, R. J., Gaziano, J. M., Darke, A. K., Crowley, J. J., Goodman, P. J., Lippman, S. M., Lad, T. E., Bearden, J. D., Goodman, G. E., Minasian, L. M., Thompson, I. M., Jr, Blanke, C. D., & Klein, E. A. (2015). Age-Related Cataract in Men in the Selenium and Vitamin E Cancer Prevention Trial Eye Endpoints Study: A Randomized Clinical Trial. *JAMA Ophthalmology*, *133*(1), 17–24. https://doi.org/10.1001/jamaophthalmol.2014.3478

14) Commission Implementing Regulation (EU) 2022/1459 of 2 September 2022 Amending Implementing Regulation (EU) 2019/804 as Regards the Terms of Authorisation of the Organic Form of Selenium Produced by Saccharomyces Cerevisiae CNCM I-3060 as Feed Additive for All Animal Species (Text with EEA Relevance), 229 OJ L (2022). http://data.europa.eu/eli/reg_impl/2022/1459/oj/eng

15) Dehkordi, A. J., Mohebbi, A., Aslani, M., & Ghoreyshi, S. (2017). Evaluation of nanoselenium (Nano-Se) effect on hematological and serum biochemical parameters of rat in experimentally lead poisoning. *Human & Experimental Toxicology*, *36*(4), 421–427. https://doi.org/10.1177/0960327116651124

16) Elkhateeb, F. S. O., Ghazalah, A. A., Lohakare, J., & Abdel-Wareth, A. A. A. (2024). Selenium nanoparticle inclusion in broiler diets for enhancing sustainable production and health. *Scientific Reports*, *14*, 18557. https://doi.org/10.1038/s41598-024-67399-7

17) Fardsadegh, B., Vaghari, H., Mohammad-Jafari, R., Najian, Y., & Jafarizadeh-Malmiri, H. (2019). Biosynthesis, characterization and antimicrobial activities assessment of fabricated selenium nanoparticles using Pelargonium zonale leaf extract. *Green Processing and Synthesis*, *8*(1), 191–198. https://doi.org/10.1515/gps-2018-0060

18) Ferroudj, A., Muthu, A., Sári, D., Törős, G., Béni, Á., Czeglédi, L., Knop, R., El-Ramady, H., & Prokisch, J. (2025). Comparative Study of Red and Grey Selenium Nanoparticles on Organ-Specific Selenium Deposition and Growth Performance in Japanese Quails. *Nanomaterials*, *15*(11), 1–14. DEENK-PA. https://doi.org/10.3390/nano15110801

19) Filipović, N., Ušjak, D., Milenković, M. T., Zheng, K., Liverani, L., Boccaccini, A. R., & Stevanović, M. M. (2021). Comparative Study of the Antimicrobial Activity of Selenium Nanoparticles With Different Surface Chemistry and Structure. *Frontiers in Bioengineering and Biotechnology*, *8*. https://doi.org/10.3389/fbioe.2020.624621

20) Gates, B., Mayers, B., Cattle, B., & Xia, Y. (2002). Synthesis and Characterization of Uniform Nanowires of Trigonal Selenium. *Advanced Functional Materials*, *12*(3), 219–227. https://doi.org/10.1002/1616-3028(200203)12:3<219::AID-ADFM219>3.0.CO;2-U

21) Gawor, A., Ruszczynska, A., Czauderna, M., & Bulska, E. (2020). Determination of Selenium Species in Muscle, Heart, and Liver Tissues of Lambs Using Mass Spectrometry Methods. *Animals : An Open Access Journal from MDPI*, *10*(5), 808. https://doi.org/10.3390/ani10050808

22) Goldan, A., Li, C., Pennycook, S., Schneider, J., Blom, A., & Zhao, W. (2016). Molecular structure of vapor-deposited amorphous selenium. *Journal of Applied Physics*, *120*. https://doi.org/10.1063/1.4962315

23) Guleria, A., Neogy, S., Raorane, B. S., & Adhikari, S. (2020). Room temperature ionic liquid assisted rapid synthesis of amorphous Se nanoparticles: Their prolonged stabilization and antioxidant studies. *Materials Chemistry and Physics*, *253*, 123369. https://doi.org/10.1016/j.matchemphys.2020.123369

24) Hadrup, N., & Ravn-Haren, G. (2023). Toxicity of repeated oral intake of organic selenium, inorganic selenium, and selenium nanoparticles: A review. *Journal of Trace Elements in Medicine and Biology*, *79*, 127235. https://doi.org/10.1016/j.jtemb.2023.127235

25) Kaewsatuan, P., Morawong, T., Lu, P., Kamkaew, A., Molee, A., & Molee, W. (2024). In ovo feeding of l-arginine and selenium nanoparticles influences post-hatch growth, muscle development, antioxidant status, and meat quality in slow-growing chickens. *Journal of Animal Science*, *102*, skae290. https://doi.org/10.1093/jas/skae290

26) Kazaz, S., Samaha, M., Hafez, M., Shobokshy, S., & Wirtu, G. (2020). Dietary supplementation of nano-selenium improves reproductive performance, sexual behavior and deposition of selenium in the testis and ovary of Japanese quail. *Journal of Advanced Veterinary and Animal Research*, *7*(4), 597. https://doi.org/10.5455/javar.2020.g457

27) Khalid, A., Tran, P. A., Norello, R., Simpson, D. A., O'Connor, A. J., & Tomljenovic-Hanic, S. (2016). Intrinsic fluorescence of selenium nanoparticles for cellular imaging applications. *Nanoscale*, *8*(6), 3376–3385. https://doi.org/10.1039/C5NR08771F

28) Khandsuren, B., & Prokisch, J. (2021a). Preparation of red and grey elemental selenium for food fortification. *Acta Alimentaria*, *50*(2), 289–298. https://doi.org/10.1556/066.2020.00332

29) Khandsuren, B., & Prokisch, J. (2021b). The production methods of selenium nanoparticles. *ACTA UNIV. SAPIENTIAE, ALIMENTARIA*, *14*, 14–43. https://doi.org/10.2478/ausal-2021-0002

30) Khazraei, S. K., Tabeidian, S. A., & Habibian, M. (2022). Selenium nanoparticles are more efficient than sodium selenite in reducing the toxicity of aflatoxin B1 in Japanese quail. *Veterinary Medicine and Science*, *8*(1), 254–266. https://doi.org/10.1002/vms3.650

31) Kizovský, M., Pilát, Z., Mylenko, M., Hrouzek, P., Kuta, J., Skoupý, R., Krzyžánek, V., Hrubanová, K., Adamczyk, O., Ježek, J., Bernatová, S., Klementová, T., Gjevik, A., Šiler, M., Samek, O., & Zemánek, P. (2021). Raman Microspectroscopic Analysis of Selenium Bioaccumulation by Green Alga Chlorella vulgaris. *Biosensors*, *11*(4), 115. https://doi.org/10.3390/bios11040115

32) Kralik, Z., Kralik, G., Grčević, M., Suchý, P., & Straková, E. (2012). Effects of increased content of organic selenium in feed on the selenium content and fatty acid profile in broiler breast muscle. *Acta Veterinaria Brno*, *81*(1), 31–35. https://doi.org/10.2754/avb201281010031

33) Li, K., Zhu, Y., Zhang, S., Xu, Q., & Guo, Y. (2024). Nitrate reductase involves in selenite reduction in *Rahnella aquatilis* HX2 and the characterization and anticancer activity of the biogenic selenium nanoparticles. *Journal of Trace Elements in Medicine and Biology*, *83*, 127387. https://doi.org/10.1016/j.jtemb.2024.127387

34) Loeschner, K., Hadrup, N., Hansen, M., Pereira, S. A., Gammelgaard, B., Møller, L. H., Mortensen, A., Lam, H. R., & Larsen, E. H. (2014). Absorption, distribution, metabolism and excretion of selenium following oral administration of elemental selenium nanoparticles or selenite in rats†. *Metallomics*, *6*(2), 330–337. https://doi.org/10.1039/c3mt00309d

35) Long, S., Li, Z., Dong, X., Yan, X., Liu, H., Tan, B., Zhang, S., Pan, S., Li, T., Suo, X., & Yang, Y. (2021). The Effect of Oxidized Fish Oil on the Spleen Index, Antioxidant Activity, Histology and Transcriptome in Juvenile Hybrid Grouper (♀ Epinephelus fuscoguttatus × ♂ Epinephelus lanceolatus). *Frontiers in Marine Science*, *8*. https://doi.org/10.3389/fmars.2021.779305

36) Mahmoud, R., Salama, B., Safhi, F. A., Pet, I., Pet, E., & Ateya, A. (2024). Assessing the Impacts of Different Levels of Nano-Selenium on Growth Performance, Serum Metabolites, and Gene Expression in Heat-Stressed Growing Quails. *Veterinary Sciences*, *11*(6), Article 6. https://doi.org/10.3390/vetsci11060228

37) Malik, Z., Marghazani, I. B., Chachar, B., Shah, Q. A., Shah, T., Mengal, B., Ujjan, N. A., & Bilal, M. (2025). Exploring the Nutraceutical Role of Selenium Nanoparticles on Laying Performance, Egg Attributes and Immune Response in Laying Hens. *Indus Journal of Bioscience Research*, *3*(5), 524–531. https://doi.org/10.70749/ijbr.v3i5.1365

38) Marković, R., Ćirić, J., Starčević, M., Šefer, D., & Baltić, M. Ž. (2018). Effects of selenium source and level in diet on glutathione peroxidase activity, tissue selenium distribution, and growth performance in poultry. *Animal Health Research Reviews*, *19*(2), 166–176. https://doi.org/10.1017/S1466252318000105

39) McFarland, L. Z., Winget, C. M., Wilson, W. O., & Johnson, C. M. (1970). Role of Selenium in Neural Physiology of Avian Species: 1. The Distribution of Selenium in Tissues of Chickens, Turkeys and Coturnix. *Poultry Science*, *49*(1), 216–221. https://doi.org/10.3382/ps.0490216

40) Mohapatra, P., Swain, R. K., Mishra, S. K., Behera, T., Swain, P., Mishra, S. S., Behura, N. C., Sabat, S. C., Sethy, K., Dhama, K., & Jayasankar, P. (2014). Effects of Dietary Nano-Selenium

on Tissue Selenium Deposition, Antioxidant Status and Immune Functions in Layer Chicks. *International Journal of Pharmacology*, *10*(3), 160–167. https://doi.org/10.3923/ijp.2014.160.167

41) National Research Council. (1994). *Subcommittee on Poultry Nutrition. (1994). Nutrient requirements of poultry: 1994. National Academies Press.* https://books.google.com/books?hl=en&lr=&id=bbV1FUqRcM0C&oi=fnd&pg=PT13&dq=national+research+council+1994+&ots=IlhS0yesUz&sig=1uUa-csTh0jrbTHUjEpJVd3Eeis

42) Reda, F. M., Alagawany, M., Salah, A. S., Mahmoud, M. A., Azzam, M. M., Di Cerbo, A., El-Saadony, M. T., & Elnesr, S. S. (2024). Biological Selenium Nanoparticles in Quail Nutrition: Biosynthesis and its Impact on Performance, Carcass, Blood Chemistry, and Cecal Microbiota. *Biological Trace Element Research*, *202*(9), 4191–4202. https://doi.org/10.1007/s12011-023-03996-3

43) Ren, L., Zhang, H., Tan, P., Chen, Y., Zhang, Z., Chang, Y., Xu, J., Yang, F., & Yu, D. (2004). Hexagonal Selenium Nanowires Synthesized via Vapor-Phase Growth. *The Journal of Physical Chemistry B*, *108*(15), 4627–4630. https://doi.org/10.1021/jp036215n

44) Ren, Z., Okyere, S. K., Zhang, M., Zhang, X., He, H., & Hu, Y. (2022). Glycine Nano-Selenium Enhances Immunoglobulin and Cytokine Production in Mice Immunized with H9N2 Avian Influenza Virus Vaccine. *International Journal of Molecular Sciences*, *23*(14), Article 14. https://doi.org/10.3390/ijms23147914

45) Sadeghian, S., Kojouri, G. A., & Mohebbi, A. (2012). Nanoparticles of Selenium as Species with Stronger Physiological Effects in Sheep in Comparison with Sodium Selenite. *Biological Trace Element Research*, *146*(3), 302–308. https://doi.org/10.1007/s12011-011-9266-8

46) Schiavon, M., & Pilon-Smits, E. A. H. (2017). The fascinating facets of plant selenium accumulation – biochemistry, physiology, evolution and ecology. *New Phytologist*, *213*(4), 1582–1596. https://doi.org/10.1111/nph.14378

47) Selmani, A., Matijaković Mlinarić, N., Falsone, S. F., Vidaković, I., Leitinger, G., Delač, I., Radatović, B., Nemet, I., Rončević, S., Bernkop-Schnürch, A., Vuletić, T., Kornmueller, K., Roblegg, E., & Prassl, R. (2024). Simulated Gastrointestinal Fluids Impact the Stability of Polymer-Functionalized Selenium Nanoparticles: Physicochemical Aspects. *International Journal of Nanomedicine*, *19*, 13485–13505. https://doi.org/10.2147/IJN.S483253

48) Shahzamani, K., Lashgarian, H. E., Karkhane, M., Ghaffarizadeh, A., Ghotekar, S., & Marzban, A. (2022). Bioactivity assessments of phyco-assisted synthesized selenium nanoparticles by aqueous extract of green seaweed, Ulva fasciata. *Emergent Materials*, *5*(6), 1689–1698. https://doi.org/10.1007/s42247-022-00415-6

49) Sindireva, A., Golubkina, N., Bezuglova, H., Fedotov, M., Alpatov, A., Erdenotsogt, E., Sękara, A., Murariu, O. C., & Caruso, G. (2023). Effects of High Doses of Selenate, Selenite and Nano-

Selenium on Biometrical Characteristics, Yield and Biofortification Levels of Vicia faba L. Cultivars. *Plants*, *12*(15), 2847. https://doi.org/10.3390/plants12152847

50) Song, C., Fei, Q., Shan, H., Feng, G., Cui, M., Liu, Y., & Huan, Y. (2013). A novel 2-(2-Formyl-4-methyl-phenoxy)-N-phenyl-acetamide-based fluorescence turn-on chemosensor for selenium determination with high selectivity and sensitivity. *Spectrochimica Acta Part A: Molecular and Biomolecular Spectroscopy*, *116*, 497–500. https://doi.org/10.1016/j.saa.2013.07.068

51) Tendenedzai, J. T., Chirwa, E. M. N., & Brink, H. G. (2022). Enterococcus spp. Cell-Free Extract: An Abiotic Route for Synthesis of Selenium Nanoparticles (SeNPs), Their Characterisation and Inhibition of Escherichia coli. *Nanomaterials*, *12*(4), 658. https://doi.org/10.3390/nano12040658

52) Tışlı, B., Nejati, O., Torkay, G., Giray, B., Bal-Öztürk, A., & Bakırdere, S. (2024). Microwave-Assisted Synthesis of Selenium Nanoparticles: Bioactivity Insights. *ChemistrySelect*, *9*(43), e202404483. https://doi.org/10.1002/slct.202404483

53) Tripathi, R. M., Hameed, P., Rao, R. P., Shrivastava, N., Mittal, J., & Mohapatra, S. (2020). Biosynthesis of Highly Stable Fluorescent Selenium Nanoparticles and the Evaluation of Their Photocatalytic Degradation of Dye. *BioNanoScience*, *10*(2), 389–396. https://doi.org/10.1007/s12668-020-00718-0

54) Tsekhmistrenko, O., Bityutskii, V., Tsekhmistrenko, S., Kharchyshyn, V., Tymoshok, N., & Spivak, M. (2020). *Efficiency of application of inorganic and nanopreparations of selenium and probiotics for growing young quails*.

55) Tugarova, A. V., Mamchenkova, P. V., Dyatlova, Y. A., & Kamnev, A. A. (2018). FTIR and Raman spectroscopic studies of selenium nanoparticles synthesised by the bacterium *Azospirillum thiophilum*. *Spectrochimica Acta Part A: Molecular and Biomolecular Spectroscopy*, *192*, 458–463. https://doi.org/10.1016/j.saa.2017.11.050

56) Urbankova, L., Skalickova, S., Pribilova, M., Ridoskova, A., Pelcova, P., Skladanka, J., & Horky, P. (2021). Effects of Sub-Lethal Doses of Selenium Nanoparticles on the Health Status of Rats. *Toxics*, *9*(2), 28. https://doi.org/10.3390/toxics9020028

57) Wang, J., Chen, M., Zhang, Z., Ma, L., & Chen, T. (2023). Selenium: From fluorescent probes to biomedical application. *Coordination Chemistry Reviews*, *493*, 215278. https://doi.org/10.1016/j.ccr.2023.215278

58) Wang, Y., Ma, J., Zhou, L., Chen, J., Liu, Y., Qiu, Z., & Zhang, S. (2012). Dual functional selenium-substituted hydroxyapatite. *Interface Focus*, *2*(3), 378–386. https://doi.org/10.1098/rsfs.2012.0002

59) Xi, G., Xiong, K., Zhao, Q., Zhang, R., Zhang, H., & Qian, Y. (2006). Nucleation−Dissolution−Recrystallization: A New Growth Mechanism for t-Selenium Nanotubes. *Crystal Growth & Design*, *6*(2), 577–582. https://doi.org/10.1021/cg050444c

60) Xiong, S., Xi, B., Wang, W., Wang, C., Fei, L., Zhou, H., & Qian, Y. (2006). The Fabrication and Characterization of Single-Crystalline Selenium Nanoneedles. *Crystal Growth & Design*, *6*(7), 1711–1716. https://doi.org/10.1021/cg060005t

61) Ye, R., Huang, J., Wang, Z., Chen, Y., & Dong, Y. (2022). The Role and Mechanism of Essential Selenoproteins for Homeostasis. *Antioxidants*, *11*(5), 973. https://doi.org/10.3390/antiox11050973

62) Zhou, X., & Wang, Y. (2011). Influence of dietary nano elemental selenium on growth performance, tissue selenium distribution, meat quality, and glutathione peroxidase activity in Guangxi Yellow chicken. *Poultry Science*, *90*(3), 680–686. https://doi.org/10.3382/ps.2010-00977

63) Zoidis, E., Demiris, N., Kominakis, A., & Pappas, A. C. (2014). Meta-analysis of selenium accumulation and expression of antioxidant enzymes in chicken tissues. *Animal*, *8*(4), 542–554. https://doi.org/10.1017/S1751731113002395

8. PUBLICATIONS

UNIVERSITY of DEBRECEN

UNIVERSITY AND NATIONAL LIBRARY
UNIVERSITY OF DEBRECEN
H-4002 Egyetem tér 1, Debrecen
Phone: +3652/410-443, email: publikaciok@lib.unideb.hu

Registry number: DEENK/214/2026.PL
Subject: PhD Publication List

Candidate: Aya Ferroudj
Doctoral School: Doctoral School of Animal Husbandry
MTMT ID: 10085943

List of publications related to the dissertation

Foreign language scientific articles in Hungarian journals (1)

1. **Ferroudj, A.**, Muthu, A., Sári, D., Seresné Törős, G., Béni, Á., El-Ramady, H., Prokisch, J.: Developing an egg model for selenium nanoparticle testing.
Acta Aliment. 2025, 1-10, 2025. ISSN: 0139-3006.
DOI: http://dx.doi.org/https://doi.org/10.1556/066.2025.00125
IF: 1 (2024)

Foreign language scientific articles in international journals (5)

2. **Ferroudj, A.**, Csik, A., Prokisch, J.: Allotrope-Dependent Physicochemical and Optical Properties of Red and Grey Selenium Nanoparticles.
RSC Adv. 22 (16), 1-8, 2026. ISSN: 2046-2069.
DOI: https://doi.org/10.1039/D6RA01409G
IF: 4.6 (2024)

3. **Ferroudj, A.**, El-Ramady, H., Prokisch, J.: Applications of Nano-Selenium in the Poultry Industry: An Overview.
Nanomaterials. 16 (2), 1-24, 2026. ISSN: 2079-4991.
DOI: https://doi.org/10.3390/nano16020142
IF: 4.3 (2024)

4. **Ferroudj, A.**, Muthu, A., Sári, D., Seresné Törős, G., Béni, Á., Czeglédi, L., Knop, R., El-Ramady, H., Prokisch, J.: Comparative Study of Red and Grey Selenium Nanoparticles on Organ-Specific Selenium Deposition and Growth Performance in Japanese Quails.
Nanomaterials. 15 (11), 1-14, 2025. ISSN: 2079-4991.
DOI: https://doi.org/10.3390/nano15110801
IF: 4.3 (2024)

5. **Ferroudj, A.**, Muthu, A., Pesti-Asbóth, G., Sári, D., Seresné Törős, G., Béni, Á., Czeglédi, L., Knop, R., El-Ramady, H., Prokisch, J.: Dietary Red and Grey Selenium Nanoparticles: Effects on Tissue Selenium Distribution, Antioxidant Capacity, and Retention in Japanese Quails.
Antioxidants. 15 (1), 1-17, 2025. EISSN: 2076-3921.
DOI: https://doi.org/10.3390/antiox15010004
IF: 6.6 (2024)

6. **Ferroudj, A.**, Semsey, D., Sári, D., Prokisch, J.: Effect of Red and Grey Selenium Nanoparticles on Yeast Growth: Short Communication.
Foods. 14 (24), 1-10, 2025. EISSN: 2304-8158.
DOI: http://dx.doi.org/10.3390/foods14244229
IF: 5.1 (2024)

Foreign language abstracts (4)

7. **Ferroudj, A.**, Prokisch, J.: From Structure to Bioactivity: Exploring Red and Grey Selenium Nanoparticles in Yeast Systems.
In: Doktoranduszok Tudományos Szimpóziuma 2026: Tudomány határok nélkül: Report of Abstracts, DOSZ, Budapest, , 2026.

8. **Ferroudj, A.**, Muthu, A., Sári, D., Seresné Törős, G., Béni, Á., Czeglédi, L., Knop, R., El-Ramady, H., Prokisch, J.: Impact of Red and Grey Nano-Selenium Supplementation on Growth and Feed Efficiency in Japanese quails.
In: Fostering the Transition to Sustainable Food Systems: Embracing Novelty and Overcoming Challenges : abstracts book

9. **Ferroudj, A.**, Muthu, A., Sári, D., Béni, Á., Czeglédi, L., Knop, R., Prokisch, J.: Spectroscopic characterization of nano-selenium and its dietary effects on quail growth and organ selenium uptake.
In: Book of abstracts of the 30th International Conference Krmiva 2025/ Zvonko Antunovic, Zlatko Janjecic, Krmiva d.o.o. Zagreb, Zagreb, , 2025, (ISSN 1847-2370)

10. **Ferroudj, A.**, Prokisch, J.: Organ-specific disposition of selenium nanoparticles in adult Japanese quails: ef fects of dietary supplementation.
In: IX. Gödöllői Állattenyésztési Tudományos Nap: Előadások és poszterek összefoglaló kötete = 9th Scientific Day of Animal Breeding in Gödöllő : Book of Abstracts of Presentations and Posters /szerk. Bényi Erzsébet, Bodnár Ákos, Pajor Ferenc, Póti Péter, Magyar Agrár- és Élettudományi Egyetem Szent István Campus, Gödöllő, 93, 2024. ISBN: 9789636231064

List of other publications

Foreign language scientific articles in international journals (16)

11. Seresné Törős, G., Alibrahem, W., Helu, N. K., Jevcsák, S., **Ferroudj, A.**, Prokisch, J.: Acrylamide in Food: From Maillard Reaction to Public Health Concern.
Toxics. 14 (2), 1-23, 2026. EISSN: 2305-6304.
DOI: http://dx.doi.org/10.3390/toxics14020110
IF: 4.1 (2024)

12. Muthu, A., Nguyen, H. H. D., Neji, C., **Ferroudj, A.**, Prokisch, J., El-Ramady, H., Béni, Á.: Determination of hydride-generated selenium in aqueous matrices by modified atomic fluorescence spectrometry.
J. Food Compos. Anal. 153, 1-10, 2026. ISSN: 0889-1575.
DOI: http://dx.doi.org/10.1016/j.jfca.2026.109169
IF: 4.6 (2024)

13. Seresné Törős, G., Atieh, R., **Ferroudj, A.**, Semsey, D., Tóth, F. A., Nagy, P. T., Prokisch, J.: Formation of Water-Soluble Fluorescent Fractions During Thermal Processing of β-Glucan-Rich Medicinal Mushrooms.
Appl. Sci.-Basel. 16 (8), 1-20, 2026. ISSN: 2076-3417.
DOI: https://doi.org/10.3390/app16083902
IF: 2.5 (2024)

14. Muthu, A., Nguyen, H. H. D., **Ferroudj, A.**, Prokisch, J., El-Ramady, H., Neji, C., Béni, Á.: Green Synthesised Carbon Nanodots Using the Maillard Reaction for the Rapid Detection of Elemental Selenium in Water and Carbonated Beverages.
Nanomaterials. 15 (15), 1-16, 2025. ISSN: 2079-4991.
DOI: http://dx.doi.org/10.3390/nano15151161
IF: 4.3 (2024)

15. Muthu, A., Nguyen, H. H. D., Neji, C., Seresné Törős, G., **Ferroudj, A.**, Atieh, R., Prokisch, J., El-Ramady, H., Béni, Á.: Nanomaterials for Smart and Sustainable Food Packaging: Nano-Sensing Mechanisms, and Regulatory Perspectives.
Foods. 14 (15), 2-29, 2025. EISSN: 2304-8158.
DOI: https://doi.org/10.3390/foods14152657
IF: 5.1 (2024)

16. Seresné Törős, G., Béni, Á., Balláné Kovács, A., Semsey, D., **Ferroudj, A.**, Prokisch, J.: Production of Myco-Nanomaterial Products from Pleurotus ostreatus (Agaricomycetes) Mushroom via Pyrolysis.
Pharmaceutics. 17 (5), 1-19, 2025. EISSN: 1999-4923.
DOI: https://doi.org/10.3390/pharmaceutics17050591
IF: 5.5 (2024)

17. Prokisch, J., **Ferroudj, A.**, Labidi, S., El-Ramady, H., Brevik, E. C.: Biological Nano-Agrochemicals for Crop Production as an Emerging Way to Address Heat and Associated Stresses.
Nanomaterials. 14 (15), 1-24, 2024. ISSN: 2079-4991.
DOI: http://dx.doi.org/10.3390/nano14151253
IF: 4.3

18. Prokisch, J., Nguyen, H. H. D., Muthu, A., **Ferroudj, A.**, Singh, A., Agrawal, S., Rajput, V. D., Ghazaryan, K., El-Ramady, H., Rai, M.: Carbon Nanodot-Microbe-Plant Nexus in Agroecosystem and Antimicrobial Applications.
Nanomaterials. 14 (15), 1-37, 2024. ISSN: 2079-4991.
DOI: http://dx.doi.org/10.3390/nano14151249
IF: 4.3

19. Sári, D., **Ferroudj, A.**, Semsey, D., El-Ramady, H., Faizy, S. E. D. A., Ibrahim, S., Mansour, H., Brevik, E. C., Solberg, S. Ø., Prokisch, J.: Drought Stress Under a Nano-Farming Approach: A Review.
Egypt. J. Soil Sci. 64 (1), 135-151, 2024. ISSN: 0302-6701.
DOI: http://dx.doi.org/10.21608/ejss.2023.239634.1668
IF: 3.4

20. Sári, D., **Ferroudj, A.**, Semsey, D., El-Ramady, H., Abowaly, M., Fawzy, Z., Mansour, H., Eid, Y., Prokisch, J.: Is Nano-Management a Sustainable Solution for Mitigation of Climate Change under the Water-Energy-Food Nexus?
Egypt. J. Soil Sci. 64 (1), 1-24, 2024. EISSN: 2357-0369.
DOI: http://dx.doi.org/10.21608/ejss.2023.233939.1656
IF: 3.4

21. Prokisch, J., Seresné Törős, G., Nguyen, H. H. D., Neji, C., **Ferroudj, A.**, Sári, D., Muthu, A., Brevik, E. C., El-Ramady, H.: Nano-Food Farming: Toward Sustainable Applications of Proteins, Mushrooms, Nano-Nutrients, and Nanofibers.
Agron. J. 14, 1-30, 2024. ISSN: 0002-1962.
DOI: http://dx.doi.org/https://doi.org/10.3390/agronomy14030606
IF: 2

22. Sári, D., **Ferroudj, A.**, Semsey, D., El-Ramady, H., Brevik, E. C., Prokisch, J.: Tellurium and Nano-Tellurium: Medicine or Poison?
Nanomaterials. 14 (8), 1-24, 2024. ISSN: 2079-4991.
DOI: http://dx.doi.org/10.3390/nano14080670
IF: 4.3

23. Muthu, A., Sári, D., **Ferroudj, A.**, El-Ramady, H., Béni, Á., Badgar, K., Prokisch, J.: Microbial-Based Biotechnology: Production and Evaluation of Selenium-Tellurium Nanoalloys.
Appl. Sci.-Basel. 13 (21), 1-14, 2023. ISSN: 2076-3417.
DOI: http://dx.doi.org/10.3390/app132111733
IF: 2.5

24. Sári, D., **Ferroudj, A.**, Muthu, A., Béni, Á., Jamalifard, R., Prokisch, J., El-Ramady, H., Elsakhawy, T., Omara, A. E. D., Brevik, E. C.: Nano-Enabled Agriculture Using Nano-Selenium for Crop Productivity: What Should be Addressed More?
EBSS. 7, 85-99, 2023. EISSN: 2536-9423.
DOI: http://dx.doi.org/10.21608/jenvbs.2023.205664.1215

25. El-Ramady, H., Abdalla, N., Sári, D., **Ferroudj, A.**, Muthu, A., Prokisch, J., Fawzy, Z., Brevik, E. C., Solberg, S. Ø.: Nanofarming: Promising Solutions for the Future of the Global Agricultural Industry.
Agronomy-Basel. 13 (6), 1-32, 2023. EISSN: 2073-4395.
DOI: http://dx.doi.org/10.3390/agronomy13061600
IF: 3.3

26. Sári, D., **Ferroudj, A.**, Abdalla, N., El-Ramady, H., Dobránszki, J., Prokisch, J.: Nano-Management Approaches for Salt Tolerance in Plants under Field and In Vitro Conditions.
Agronomy-Basel. 13 (11), 1-27, 2023. EISSN: 2073-4395.
DOI: http://dx.doi.org/10.3390/agronomy13112695
IF: 3.3

Foreign language abstracts (1)

27. Muthu, A., **Ferroudj, A.**, Sári, D., Béni, Á., El-Ramady, H., Prokisch, J.: Production methods for making nano Selenium, nano Tellurium and nano alloys, as potential materials in the food and pharma industry.
In: Táplálkozástudományi Kutatások : XI. PhD konferencia programja és az előadások összefoglalói. Szerk.: Bíró Lajos, Gelencsér Éva, Lugasi Andrea, Rurik Imre, Simonné Sarkadi Livia, Magyar Táplálkozástudományi Társaság, Budapest, 13, 2023. ISBN: 9786155606144

Total IF of journals (all publications): 82,8
Total IF of journals (publications related to the dissertation): 25,9

The Candidate's publication data submitted to the Tudóstér have been validated by DEENK on the basis of the Journal Citation Report (Impact Factor) database.

23 April, 2026